METAMODELLING OF STIFFNESS MATRICES FOR 2D WELDED ASYMMETRIC STEEL JOINTS

Alfonso Loureiro [a,*], Manuel Lopez [a], J.Manuel Reinosa [a], Ruth Gutierrez [a], Eduardo Bayo [b]

a University of A Coruña, Spain

b University of Navarra, Spain

This is a post-peer-review, pre-copyedit version of an article published in Engineering Structures.

The final authenticated version is available online at:

https://doi.org/10.1016/j.engstruct. 2019.105703

ABSTRACT

Beam-column steel joints usually have a semi-rigid behaviour, and this must be taken into account when carrying out a global analysis of the structure. Rotational springs at each side of the joint are commonly used to simulate this behaviour by means of the component method, but asymmetric welded beam-column steel joints are not included in the formulations of Eurocode 3. This research work proposes a new methodology to obtain the stiffness of welded asymmetrical beam-column steel joints, by means of a cruciform element of 4 nodes and 12 DOF, whose stiffness matrix is directly obtained by means of the meta-modelling of its elements using Kriging´s method. The authors have carried out a wide study of 754 different asymmetric welded beam-column steel joints, whose finite element models have been analysed, and then the static condensation method has been used to obtain the equivalent condensed stiffness matrix (Kcond) of the cruciform element for the joints belonging to the training set. These matrices have been used to build the Kriging's model, and the rest of joints have been used for testing the method, which yields very good results. The use of meta-modelling methods to obtain the stiffness matrix of the joint is not only easier in its application than the *component* method, but it also leads to a formulation that is more accurate, and also takes into account the interactions between the different parts of the joint.

1. INTRODUCTION

Beam-column steel joints usually have a semi-rigid behaviour, and this must be taken into account when carrying out a global analysis of the structure, as established in current structural design steel codes, and more specifically in Eurocode 3 [1-2]. Rotational springs at each side of the joint are commonly used to simulate this behaviour in a global analysis [2-4]. Eurocode 3, part 1-8 [2], establishes the *component* method, as an instrument to determine the stiffness of the joints. The method consists of dividing the joint into its different resistant elements, such as: the column web in shear, the column web under compression and tension, column flanges in bending, bolts in tension, beam flanges in

tension and compression, etc. Many researchers have been working in recent years to determine the stiffness and resistance of each of these components. In this respect, some authors have emphasized the importance of the column web when determining the stiffness of the joint [5-7], and new components have been developed to characterize the stiffness of the column web under shear for joints with beams of unequal depth (asymmetric joints) [8-10]. However, the direct use of the components attached to rigid bars in mechanical models has a high computational cost when performing the global analysis. In order to circumvent this problem Bayo et al. [11] have proposed the use of 12 degree of freedom (DOF) cruciform finite elements for global analysis. In addition, it has been demonstrated in works such as [12-13] the good performance of the finite element models when characterizing the behaviour of both steel and composite joints.

Therefore, there has been an important advance in the knowledge of the behaviour of beam-column joints in general. However, the practical application of the component method is not easy due to several reasons. One of them is undoubtedly the impossibility of the method to take into account some of the interactions between the different components of the joint. Another difficulty arises when analysing joints with non-symmetric configurations. In fact, asymmetric welded beam-column steel joints are not included in the formulations of Eurocode 3. And finally, the component method becomes impractical in the case of 3D joints due mainly to the extreme difficulty in assessing the interactions among all the components. In this sense, Loureiro et al [14] have studied the influence between the load levels of the weak axis and the stiffness of the strong axis for 3D bolted joints, showing that the interaction between the load levels of both axes cannot be neglected. Similar conclusions have been reached recently by Costa et al [15]. It is therefore necessary to look for new ways to consider the stiffness and resistance of joints in the global analysis of the structure. In this sense, one of the objectives of this research is to provide a new methodology to obtain the stiffness of welded asymmetrical steel joints.

Research leading to the use of meta-modelling methods to determine the behaviour of joints has been proposed in recent works. Díaz et al. [16] proposed a methodology for the optimal design of semi-rigid steel connections using meta-models generated with Kriging and Latin Hypercube, and optimized using the genetic algorithms. This methodology was applied to two examples involving bolted extended end-plate connections with good results. Anderson et al. [17] have performed a series of tests, in which significant parameters have been systematically varied. The results have been used to train an artificial neural network (ANN) to predict bi-linear moment-rotation characteristics for minor-axis connections. The results were satisfactory for their use in structural engineering design. De Lima et al. [18] proposed the use of artificial neural networks to predict the flexural resistance and initial stiffness of beam-to-column steel joints using the back propagation supervised learning algorithm, for three types of steel beam-to-column joints: welded, end plate and bolted with top, seat and double web angles, respectively. The neural networks results proved to be consistent with experimental and design code reference values. Guzelbey et al. [19] proposed Neural Networks for the estimation of available rotation capacity of wide flange beams. The results of the NN approach were compared with numerical FE models and the method was more practical and faster than the FE models.

Kriging's method [20] has recently been used by Bayo and Gracia [21] in an interesting work to build a surrogate model of the stiffness matrix of cruciform elements of 12 DOF for symmetrical welded joints (beams of equal depth at both sides of the column). The stiffness matrices of the training set points were obtained by means of detailed finite element models that were subsequently condensed to the 12 DOF of the cruciform element. The properties of the joints were characterized by means of meta-modelling the deformation modes of the joints and their corresponding eigenvalues. However, this methodology cannot be extended to asymmetric beam-column joints due to the complexity of the problem when determining and classifying the deformation modes of

the joint. This complexity is due precisely to their asymmetry. The use of meta-modelling methods to obtain the stiffness matrix of the joint is not only easier in its application than the component method, but it also leads to a formulation that is more accurate, and also takes into account the interactions between the different parts of the joint. In addition, this methodology could be extended to 3D joints.

What is proposed in this paper, is to accurately model the joint by a cruciform element of 4 nodes and 12 DOF, whose stiffness matrix is directly obtained by means of the meta-modelling of its elements using Kriging´s method. The authors have carried out a wide study of 754 different asymmetric welded steel joints, whose results are showed in the next paragraphs.

2. FINITE ELEMENT MODELS

To achieve the final objective of this work, it has been necessary to carry out a wide parametric analysis. In order to perform the parametric analysis, calibrated finite element models have been used based on the tests and models developed in a previous work of Loureiro et al. [22], from which the web stiffeners have been removed. The extensive previous experience in the finite element analysis of this type of models, allows ensuring the correctness of the finite element models without the need of carrying out additional tests. A total of 754 asymmetric beam-column joints have been analysed using detailed finite element models. 377 of them have a hot rolled HEA column and the other 377 have a HEB column. The beams are hot rolled IPE in all cases. The column profiles used for the study range from HEA and HEB 100 to HEA and HEB 400, and the beam profiles go from IPE 80 to IPE 600.

The columns were combined with the beams according to the following criteria: for each column, the greater beam whose flange fits in the column has been taken. This beam (left beam) is placed on the left part of the joint, and has been combined with several beams of smaller heights (right beams) on the right side of the column, to span a reasonable combination of possible cases. Subsequently the left beams were reduced, and again combined with several beams on the right side of the joint. This process has been repeated until a reasonable lower limit on the size of the left beam.

As an example, Table 1 shows the combinations corresponding to the column HEA 200. In this case, the left beam goes from IPE 500 to IPE 360, and the right beams vary from IPE 450 to IPE 240, with a total of 22 different configurations.

Column	Left Beam	Right Beam		Column	Left Beam	Right Beam
HE 200 A	IPE 500	IPE 240		HE 200 A	IPE 450	IPE 360
HE 200 A	IPE 500	IPE 270		HE 200 A	IPE 450	IPE 400
HE 200 A	IPE 500	IPE 300		HE 200 A	IPE 400	IPE 240
HE 200 A	IPE 500	IPE 330		HE 200 A	IPE 400	IPE 270
HE 200 A	IPE 500	IPE 360		HE 200 A	IPE 400	IPE 300
HE 200 A	IPE 500	IPE 400		HE 200 A	IPE 400	IPE 330
HE 200 A	IPE 500	IPE 450		HE 200 A	IPE 400	IPE 360
HE 200 A	IPE 450	IPE 240		HE 200 A	IPE 360	IPE 240
HE 200 A	IPE 450	IPE 270		HE 200 A	IPE 360	IPE 270
HE 200 A	IPE 450	IPE 300		HE 200 A	IPE 360	IPE 300
HE 200 A	IPE 450	IPE 330		HE 200 A	IPE 360	IPE 330

Table 1. Joint configurations for the HEA200 column.

Each of these 754 joints has been modelled by means of the finite element program Abaqus® , using C3D8R elements. Symmetry conditions with respect to the middle plane of the joint web have been applied, as shown in Figure 1. S275 steel has been introduced in the modelling by means of a linear elastic stress-strain curve. A Young modulus of 2.1E5 N/mm^2 and a Poisson ratio of 0.3 have been adopted. Rigid surfaces have been situated in the 4 faces of the joints. In each of these surfaces, a reference point (with 3 DOF: 2 translations and 1 rotation) has been situated with the aim of obtaining the stiffness matrix condensed to 12 DOF. The analysis of the joints has been done by means of a Python subroutine. For each of the joints, the geometry read from a previous database has been generated, and then the condensed matrix has been extracted and saved in a text file. This process has been repeated until all the joints have been analysed. As a consequence, at the end of the process, a text file with 754 condensed matrices has been obtained. The number of elements and nodes is not the same for all the models, with an average value of 17,736 elements and 24,944 nodes per model. The type of analysis implicit in the static condensation algorithm is linear elastic, and the average processing time has been around 15 seconds per joint.

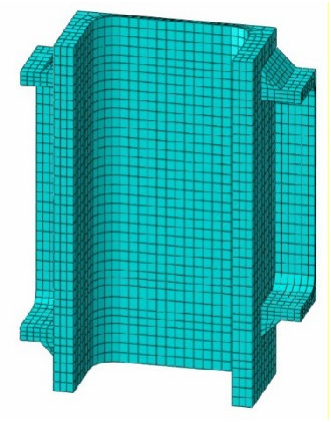

Figure 1. Finite element model of the joint

3. PROCEDURE FOR OBTAINING THE CONDENSED STIFFNESS MATRIX OF THE JOINT

As indicated in the previous paragraphs, the objective of the work is to model the joint by a cruciform element of 4 nodes and 12 DOF (see Figure 2a), whose stiffness matrix is obtained through a meta-modelling of its components using Kriging's method. For the cases belonging to the training set the static condensation method has been used to obtain the equivalent condensed stiffness matrix (*Kcond*) of the cruciform element. The joints have been cut at a distance of 10 mm from the fillet weld (see Figure 2b). The complete stiffness matrix of the finite element model contains several thousands of DOF, and static condensation requires the following process.

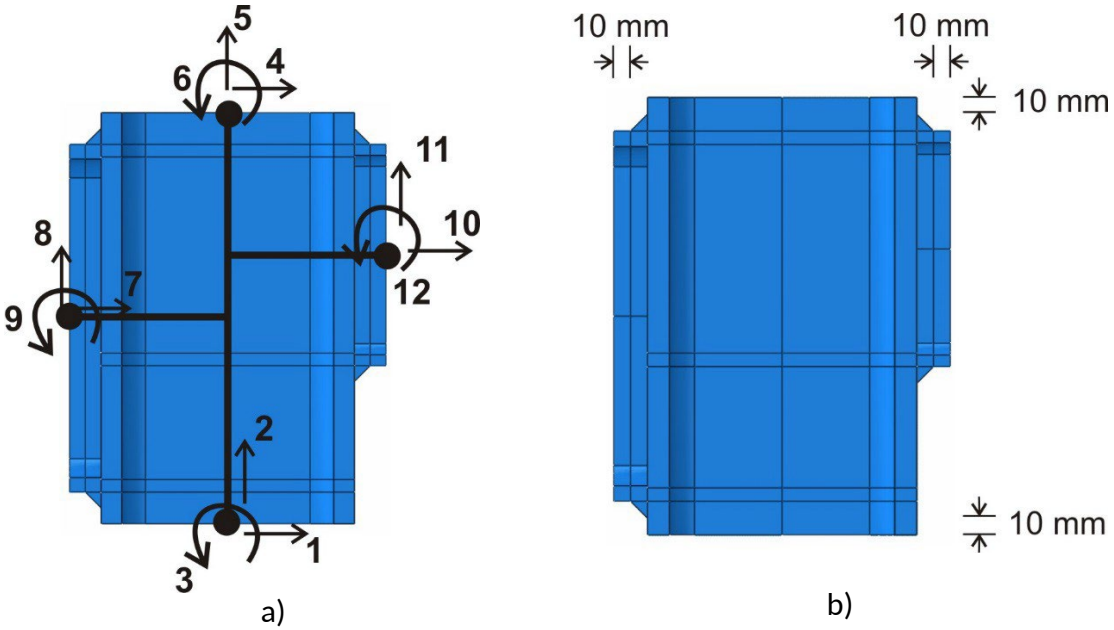

a) b)

Figure 2. Degrees of freedom of the cruciform element (a) and dimensions of the joint (b)

After a reordering of the degrees of freedom the following procedure of static condensation has been applied.

$$\begin{bmatrix} Rc \\ Re \end{bmatrix} = \begin{bmatrix} Kcc & Kce \\ Kec & Kee \end{bmatrix} \begin{bmatrix} Dc \\ De \end{bmatrix} \quad (1)$$

where:

Rc = Force vector of the master DOF to condense.

Re = Force vector corresponding to the DOF to be condensed out.

Dc = Master displacements (12 DOF).

De = Displacement vector for the DOF to eliminate or condense out.

Then, taking into account that the external forces *Re* are null (*Re* = *0*), and operating:

$$Re = Kec.Dc + Kee.De = 0 \rightarrow De = -Kee^{-1}.Kec.Dc \quad (2)$$

$$Rc = Kcc.Dc + Kce.De \rightarrow Rc = \left[Kcc - Kce\left(Kee^{-1}.Kec\right)\right]Dc \quad (3)$$

And therefore, the condensed stiffness matrix of the joint can be written as:

$$Kcond = Kcc - Kce\left(Kee^{-1}.Kec\right) \quad (4)$$

In the present work, the software Abaqus® has been used to obtain $Kcond$ by means of a "substructure" analysis as explained in Bayo and Gracia [21].

This static condensation procedure has been carried out for all the analysed cases that form the training and validation sets, leading to a database of 754 condensed stiffness matrices, 377 for the HEA and 377 for the HEB column models. As indicated above, the condensed matrices are symmetric, and therefore the total number of components to be determined in the meta-modelling process is 78.

4. COMPARISON BETWEEN Kcond AND FEM.

In order to verify the correct performance of the cruciform element with the condensed stiffness matrix, the frame whose dimensions and DOF are shown in Figure 3 has been analysed. Four different joints have been studied, which are indicated in Table 2.

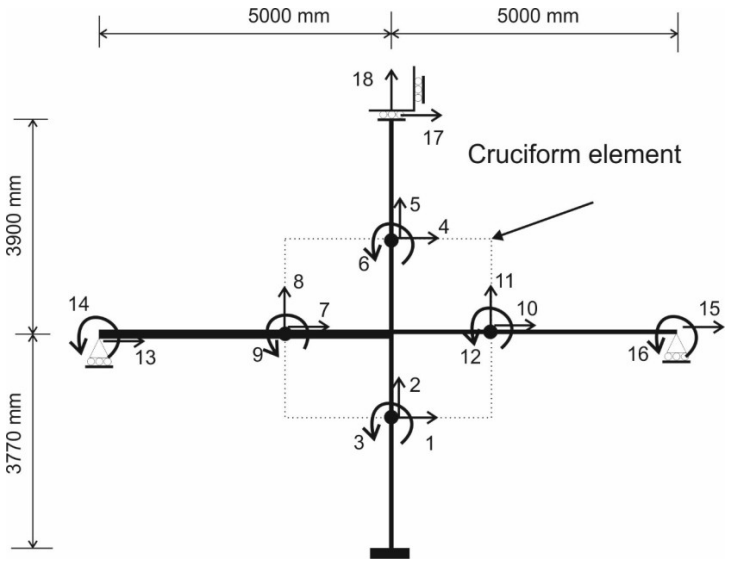

Figure 3. Dimensions and DOF for the example frame.

Model	Column	Left beam	Right beam
1	HEB200	IPE400	IPE300
2	HEB240	IPE500	IPE360
3	HEA200	IPE400	IPE300
4	HEA240	IPE500	IPE360

Table 2. Configuration of the cross frames.

The frame is formed by a column of 7670 mm, with two beams of different height on both sides. The lengths of the beams are 5000 mm, and they connect to the column at a height of 3770 mm from the lower end. The column is fully fixed in its lower end. The upper end has restricted rotations, but not the horizontal and vertical displacements. The beams are simple supported in their ends with free sliding in horizontal direction.

For the evaluation of the methodology, gravity loads have been introduced in the beams, and point loads in the column and beams, simulating the loads coming from the upper floors and wind, respectively, as shown in Figure 4. The two loading combinations showed in Table 3 have been applied with a total of eight different analyses as indicated in Table 4.

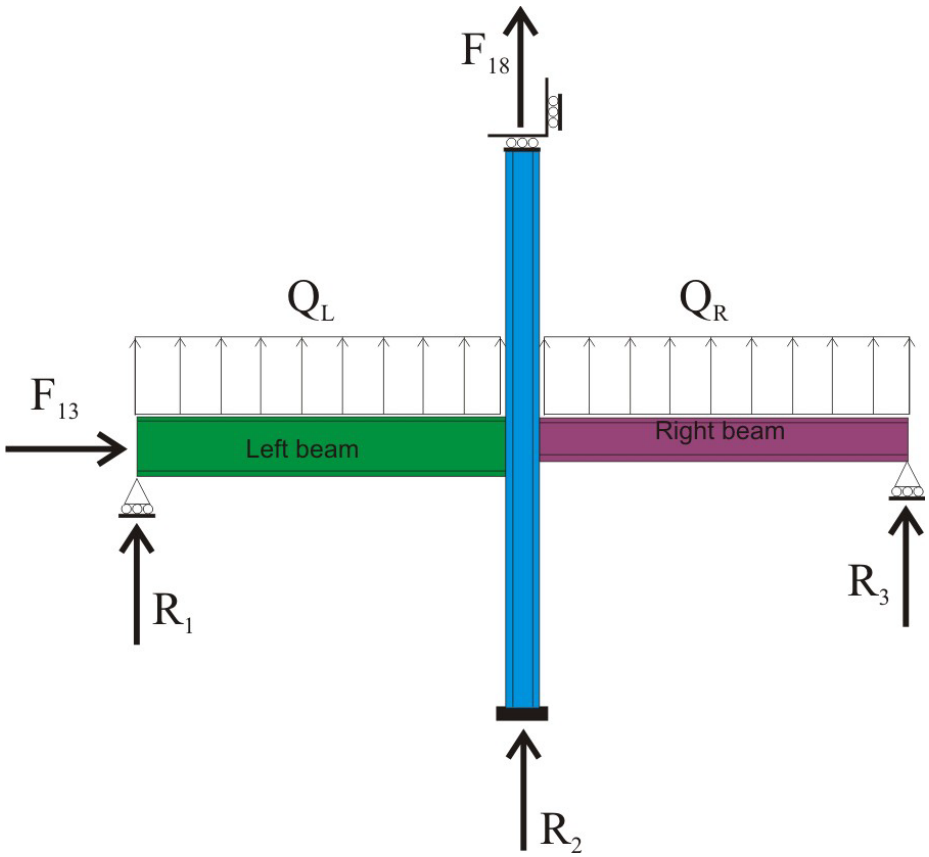

Figure 4. Illustration of the loads in the example frame

All loading cases have been modelled by means of finite elements with the commercial program Abaqus® using the model presented in Figure 5 with a total of 1.5 million DOF, and simultaneously by means of a matrix analysis implemented in Matlab®, introducing the cruciform element of the joint with the condensed stiffness matrix previously calculated. This model has a total of 18 DOF as shown in Figure 3. The finite element model represents half of the complete frame, with symmetry conditions applied to the middle plane of the structure. As explained in previous sections, C3D8R solid elements with hourglass control have been used with the aim of avoiding shear locking.

In all cases, the reactions and rotations indicated in Table 4 have been extracted both from FEM and Matlab® program. The comparative results between the proposed method using the condensed stiffness matrix of the joint, and those obtained from the complete finite element model are shown in Table 4.

The percentage error has been calculated as:

$$Error(\%) = \frac{Kcond\ result - FEM\ result}{FEM\ result} * 100 \qquad (5)$$

	Q_L (KN/m)	Q_R (KN/m)	F_{13} (KN)	F_{18} (KN)
LC_A	-25	0	-10	-240
LC_B	0	-25	10	-240

Table 3. Load cases for the cross frame.

Error (%) Kcond versus FEM								
	Model 1		Model 2		Model 3		Model 4	
	LC_A	LC_B	LC_A	LC_B	LC_A	LC_B	LC_A	LC_B
fi14	0.7	8.1	-0.6	9.8	0.6	7.8	-0.4	9.2
fi9	0.3	0.1	-0.6	-1.6	-0.1	-0.3	-0.9	-2.6
fi12	1.9	-2.2	2.0	-6.1	1.7	-2.5	2.0	-7.1
fi16	6.6	-1.3	8.9	-5.3	6.6	-1.2	9.5	-6.0
R1	-1.4	0.2	-2.9	-0.6	-1.5	-0.4	-2.9	-1.8
R2	-0.9	-0.9	-2.9	-4.5	-0.9	-0.9	-2.9	-5.4
R3	1.1	-1.5	1.	-5.3	0.8	-1.5	1.3	-6.2

Table 4. Comparative results between *Kcond* method and complete FEM for the example frame.

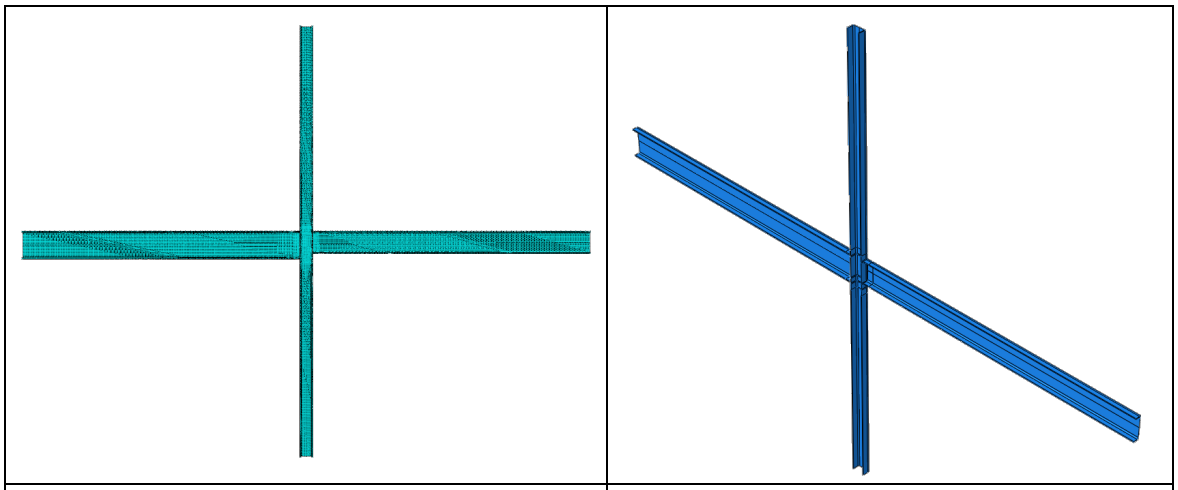

a) Frontal view of the mesh | b) Isometric view

Figure 5. Finite elements model of the cross frame

As can be seen, the cruciform element with the condensed stiffness matrix yields very good results, and therefore, it can be asserted that the condensed stiffness matrix correctly simulates the complex behaviour of the joint, taking into account all the interactions between the different parts and degrees of freedom without the need of calculating and assembling the components of such joint. As a consequence, these results justify the proposed modelling method.

5. DIRECT MODELIZATION OF THE CONDENSED STIFFNESS MATRIX.

It has been shown that the use of the condensed stiffness matrix (*Kcond*) leads to very good results, although it has a disadvantage. For each different configuration it is necessary to model the joint in Abaqus® or a similar software, and by means of the static condensation procedure, obtain the condensed stiffness matrix. This involves a significant computational and economic cost, and also may not be accessible to all designers. For this reason, what is proposed in this work is to use a meta-modelling method for obtaining in a direct way the elements of the condensed stiffness matrix. In this case, it is necessary to meta-model 78 components for each matrix, since *Kcond* is a symmetric matrix, and consequently it is enough to model the components of the diagonal and the upper triangular matrix. Kriging's method has been used by Bayo and Gracia [22] to build a surrogate model of symmetric steel joints based on the deformation modes, and their approach has yielded very good results. However, what is proposed in this present work, is the direct meta-modelling of the components of the stiffness matrix, since when dealing with asymmetric joints, the meta-modelling of the eigenvalues and eigenvectors of the condensed stiffness matrices do not follow similar patterns and their classification presents great difficulties.

Kriging's method consists of predicting the response of a system based on two parts: a regression model and a radial model. In this work we have used the implementation of DACE [20], which allows the use of regression models with constant, linear and quadratic

interpolation. The radial part allows correlation models of the following type: linear, exponential, Gaussian, spherical, cubic and spline. The parameters of the Kriging model are determined by minimizing the Mean Square Error (MSE). The variables of the joints models that have been used as inputs to the DACE model are: *ch* (column height), *cw* (column width), *tcw* (thickness of the column web), *tcf* (thickness of the column flange), *hlb* (height of the left beam) and *hrb* (height of the right beam). The weld thickness was initially included in the study as an additional variable, however it was eliminated after observing that its influence on the results was negligible. The linear regression model and the Gaussian correlation model have been used.

As indicated above, 754 joints have been modelled (377 corresponding to HEAs columns and 377 to HEBs columns), and their corresponding condensed stiffness matrices have been obtained. 76% of these matrices (285 with HEAs columns and 285 with HEBs columns) have been used as input data to train the surrogate model (training set), and the remaining 24 % connections showed in Annex 1 and Annex 2 at the end of the text (92 with HEAs columns and 92 with HEBs columns) have been used as input models for the validation set.

Subsequently, once the components of the stiffness matrix of the joints have been obtained by Kriging's method (*K_Kriging*), they have been introduced into the example frame defined in the previous sections (see Figures 3 and 4), and the results obtained have been compared with those obtained using *K_cond*. The following two load cases have been studied.

CLC1: The gravity loads on the right beam (Q_R) and the left beam (Q_L) are downward and they reach the 25% and 50%, respectively, of their corresponding maximum bending resistance considered as double pinned beams. F_{18} is a downward vertical load that reaches 75% of the maximum compression strength of the column, and F_{13} is a horizontal load to the right with a value of the 12.5% of F_{18}.

CLC2: The gravity loads on the right beam (Q_R) and the left beam (Q_L) are downward and they reach the 50% and 25%, respectively, of their corresponding maximum bending resistance considered as double pinned beams. F_{18} is a downward vertical load that reaches 75% of the maximum compression strength of the column, and F_{13} is a horizontal load to the left with a value of the 12.5% of F_{18}.

Figures 6 to 9 show a graphical comparison between the results obtained using *Kcond* and *K_Kriging*. The comparison is based on the percentage errors for the displacements, rotations and reactions indicated in Figures 3 and 4, and it can be observed that the maximum relative error is 3.60%. Table 5 show the R^2 parameter for each reaction and displacement, according with Equation (6). The closer R^2 is to 1 the greater the precision of the method.

$$R^2 = 1 - \frac{\sum_{i=1}^{n} (Ycond,i - Y\_Kriging,i)^2}{\sum_{i=1}^{n} (Ycond,i - Ycond,average)^2} \qquad (6)$$

where *i* is the model number, *n* is the number of models that has been analysed (92 both for HEAs and HEBs columns), *Ycond*,*i* is the value of the reaction or displacement obtained with the condensed stiffness matrix (*Kcond*) for the corresponding *i* model, *Y_Kriging*,*i* is the value of the reaction or displacement obtained with the Kriging stiffness matrix (*K_Kriging*) for the corresponding *i* model; and *Ycond*,*average* is the mean value of *Ycond* for each reaction or displacement.

As can be seen, the use of *K_Kriging* presents a very good agreement with respect to the use of the condensed matrix; both in what concerns to the R^2 parameter as well as the relative errors.

Table 6 shows the mean absolute percentage error (MAPE) in % calculated according to Equation (7).

$$MAPE = \frac{100}{n}\sum_{i=1}^{n}\left|\frac{Y_{cond,i} - Y_{Kriging,i}}{Y_{Kriging,i}}\right| \quad (7)$$

Table 7 shows the root mean square error (RMSE) value, calculated according to Equation (8).

$$RMSE = \sqrt{\frac{1}{n}\sum_{i=1}^{n} e_i^2} = \sqrt{\frac{1}{n}\sum_{i=1}^{n}\left(Y_{cond,i} - Y_{Kriging,i}\right)^2} \quad (8)$$

*where ei is the absolute err*or between the results obtained with the use of the FE condensed matrix and those obtained with the Kriging's method, as explained in the previous paragraphs.

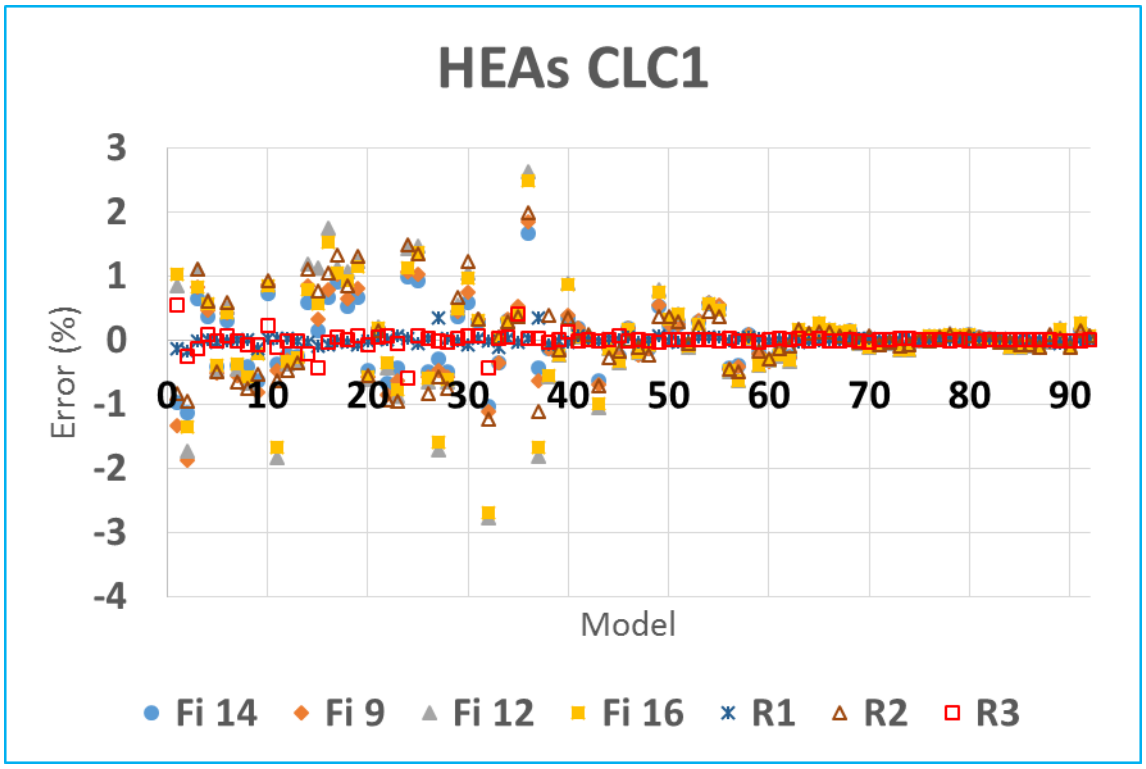

Figure 6. Rotations and Reactions relative errors for HEAs columns and load case CLC1

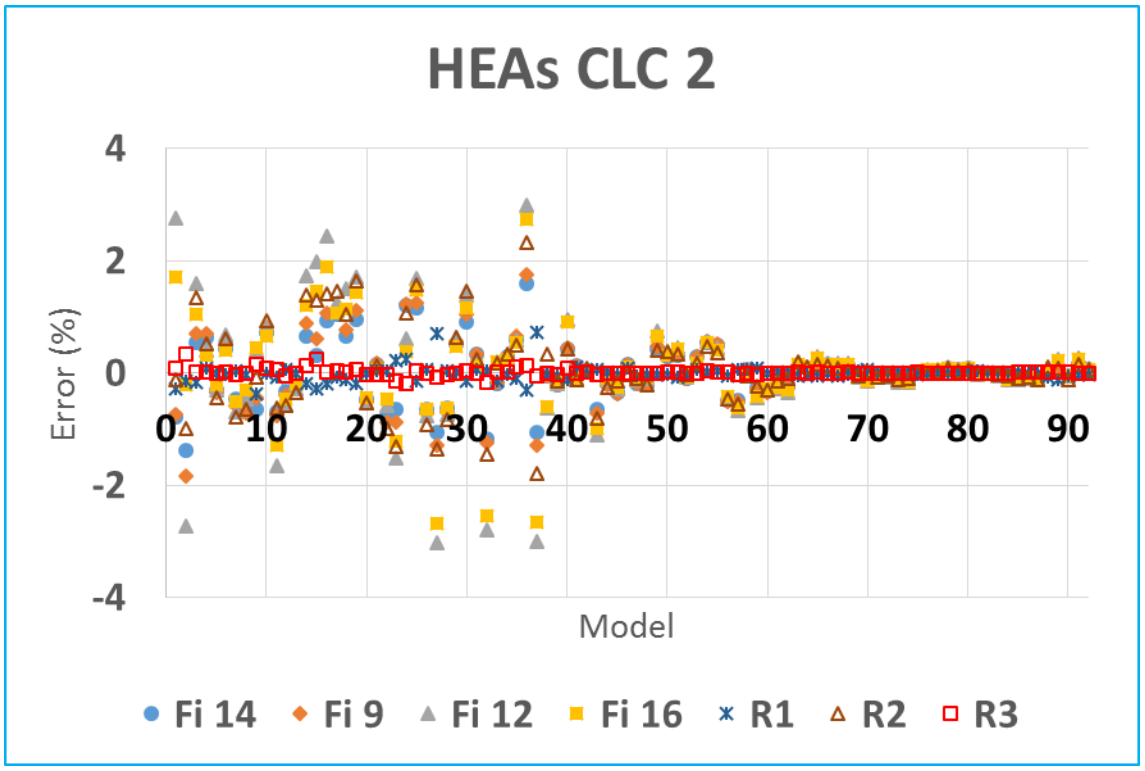

Figure 7. Rotations and Reactions relative errors for HEAs columns and load case CLC2

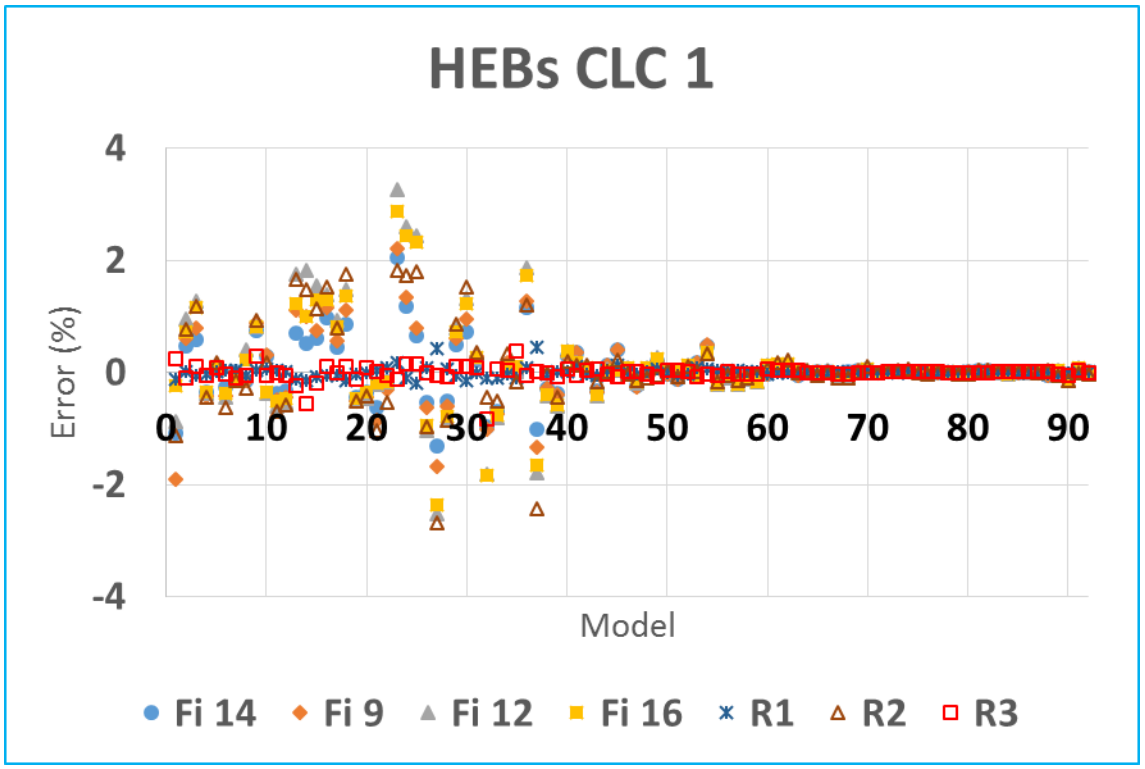

Figure 8. Rotations and Reactions relative errors for HEBs columns and load case CLC1

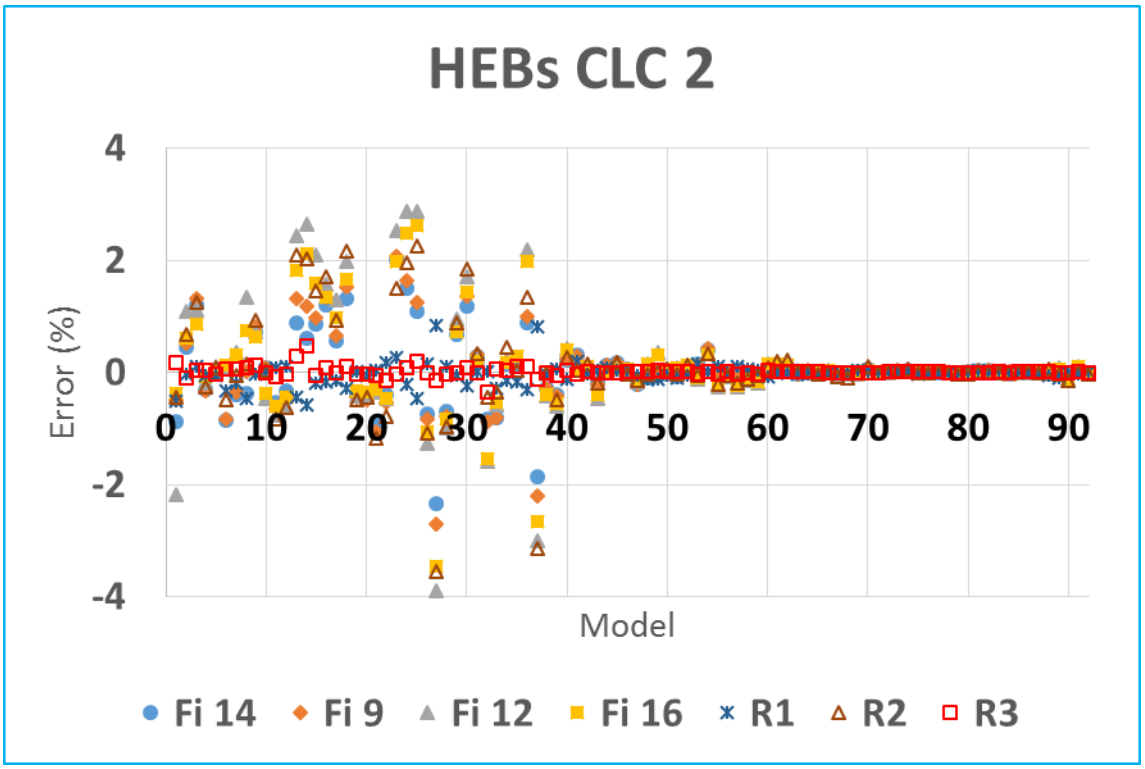

Figure 9. Rotations and Reactions relative errors for HEBs columns and load case CLC2

Table 5. R^2 parameter for reactions and rotations

	R^2 parameter			
	HEAs_CLC1	HEAs_CLC2	HEBs_CLC1	HEBs_CLC2
Fi 14	1.000	0.999	1.000	0.999
Fi 9	1.000	0.999	1.000	0.999
Fi 12	0.999	0.999	0.999	0.999
Fi 16	0.999	0.998	0.999	0.998
R1	1.000	0.998	1.000	0.998
R2	1.000	1.000	1.000	1.000
R3	0.998	1.000	0.997	1.000

Table 6. MAPE parameter for reactions and rotations

	MAPE parameter (%)			
	HEAs_CLC1	HEAs_CLC2	HEBs_CLC1	HEBs_CLC2
Fi 14	0.32	0.38	0.28	0.35
Fi 9	0.38	0.42	0.35	0.39
Fi 12	0.51	0.63	0.47	0.58
Fi 16	0.46	0.50	0.42	0.47
R1	0.03	0.08	0.05	0.11
R2	0.41	0.46	0.43	0.47
R3	0.05	0.03	0.06	0.04

Table 7. RMSE parameter for reactions and rotations

	RMSE parameter			
	HEAs_CLC1	HEAs_CLC2	HEBs_CLC1	HEBs_CLC2
Fi 14	0.0044	0.0052	0.0047	0.0060
Fi 9	0.0053	0.0059	0.0058	0.0068
Fi 12	0.0077	0.0100	0.0084	0.0104
Fi 16	0.0070	0.0080	0.0075	0.0085
R1	0.0006	0.0014	0.0008	0.0019
R2	0.0059	0.0069	0.0073	0.0086
R3	0.0012	0.0006	0.0013	0.0008

6. CONCLUSIONS

The aim of this work has been to present a new and accurate methodology for obtaining the stiffness matrix of asymmetric welded steel joints, by means of the meta-modelling of its components. 754 different joints have been analysed by detailed finite element models, and their condensed stiffness matrix corresponding to the cruciform element of 4 nodes and 12 degrees of freedom have been extracted. Structural simulation of a frame

with Matlab® and complete FE models have been performed providing a very good agreement for different load combinations. Kriging's method (DACE) has been used for the meta-modelling of the components of the condensed stiffness matrix. Both the *Kcond* extracted from FEM and the *K_Kriging* obtained by means of the proposed meta-modelling method have been introduced in the frame analysis resulting also in a very good agreement. Consequently, the following conclusions can be cited:

- It has been shown that the condensed stiffness matrices of the analysed asymmetric steel joints simulate the global behaviour of the structure with high precision, and take into account the interaction between the different degrees of freedom of the joint.
- Kriging's method leads to very good results when meta-modelling the components of the condensed stiffness matrix in a direct way. For the subrogate model 76 % of joints have been in the training set, and 24 % of joints for the validation set.
- The use of the meta-modelling method allows obtaining the stiffness matrix without the need of FE modelling of the joint and the subsequent static condensation of the matrix.
- The behaviour of asymmetric joints is not contemplated in Eurocode 3, and the use of the condensed or the Kriging matrices represents a very good alternative method for solving this important problem.
- This method allows obtaining the stiffness matrix of the joint in a very easy and fast manner, with only five parameters corresponding to the dimensions of columns and beams.
- The application of this technique to beam-column joints with bolted end plate will be studied in future works, with the aim of obtaining results as good as those obtained for welded joints. It is foreseen however, that the number of parameters necessary to correctly meta-model the behaviour of the joints will be larger, and this will increase the complexity of the models.

ACKNOWLEDGEMENTS

The financial support provided by the Spanish Ministerio de Economía y Competitividad and Fondo Europeo de Desarrollo Regional under contract BIA2016-80358-C2-2-P and BIA2016-80358-C2-1-P MINECO/FEDER UE is gratefully acknowledged.

REFERENCES

[1] CEN. Eurocode 3, Design of steel structures, Part 1.1: General Rules and Rules for Buildings, 2005, EN 1993-1-1.

[2] CEN. Eurocode 3, Design of steel structures, Part 1.8: Design of Joints, 2005, EN 1993-1-8.

[3] Frye M.J., Morris G.A., Analysis of flexible connected steel frames, Can. J. Civ. Eng. 2 (1975) 119–136.

[4] N. Kishi, W.F. Chen, Data base of steel column connections, Structural Engineering Report CE-STR-86-26, Purdue University, West Lafayette IN, 1986.

[5] H. Krawinkler, Shear in beam-column joints in seismic design of steel frames, Eng. J. AISC 5 (1978) 82–90.

[6] J.M. Castro, A.Y. Elghazouli, B.A. Izzuddin, Modelling of the panel zone in steel and composite frames, Eng. Struct. 27 (2005) 129–144.

[7] C. Faella, V. Piluso, G. Rizzano, Structural Steel Semirigid Connections: Theory, Design and Software, CRC Publishers, 2000.

[8] E. Bayo, A. Loureiro, M. Lopez, Shear behaviour of trapezoidal column panels. I: Experiments and finite element modelling, Journal of Constructional Steel Research. 108 (2015) 60–69.

[9] M. Lopez, A. Loureiro, E. Bayo, Shear behaviour of trapezoidal column panels. II: parametric study and cruciform element, Journal of Constructional Steel Research. 108 (2015) 70–81.

[10] A. Loureiro, M. Lopez, E. Bayo, Shear behaviour of stiffened double rectangular column panels: characterization and cruciform element, Journal of Constructional Steel Research. 117 (2016) 126–138.

[11] E. Bayo, J. Gracia, B. Gil, R. Goñi, An efficient cruciform element to model semi-rigid composite connections for frame analysis, Journal of Constructional Steel Research. 72 (2012) 97–104.

[12] E. Bayo, A. Loureiro, M. Lopez, L. Simões da Silva, General component based cruciform finite elements to model 2D steel joints with beams of equal and different depths, Engineering Structures. 152 (2017) 698–708.

[13] H. Augusto, L. Simões da Silva, C. Rebelo, J.M. Castro, Characterization of web panel components in double-extended bolted end-plate steel joints, Journal of Constructional Steel Research. 116 (2016) 271–293.

[14] Loureiro, A., Moreno, A., Gutiérrez, R., & Reinosa, J. M. (2012). Experimental and numerical analysis of three-dimensional semi-rigid steel joints under non-proportional loading. Engineering Structures, 38, 68–77.

[15] Costa R., Valdeza J., Oliveira S., Simões da Silva L., Bayo E. Experimental behaviour of 3D end-plate beam-to-column bolted steel joints. Engineering Structures. Vol. 188. pp. 277–289. (2019).

[16] C. Díaz,M. Victoria, O.M. Querin, P.Martí, Optimum design of semi-rigid connections using metamodels, Journal of Constructional Steel Research. 78 (2012) 97–106.

[17] D. Anderson, E.L. Hines, S.J. Arthur, E.L. Eiap, Application of artificial neural networks to the prediction of minor axis steel connections, Compututers and Structures. 63 (4) (1997) 685–692.

[18] L.R.O. De Lima, P.C.G. da S Vellasco, S.A.L. de Andrade, M.M.B.R. Vellasco, J.G.S. da Silva, Neural networks assessment of beam-to-column joints, J. Braz. Soc. Mech. Sci. Eng. 28 (3) (2005) 314–324.

[19] I.H. Guzelbey, C. Abdulkadir, T.G. Mehmet, Prediction of rotation capacity of wide flange beams using neural networks, Journal of Constructional Steel Research. 62 (10) (2006) 950–961.

[20] S.N. Lophaven, H.B. Nielsen, J. Søndergaard, DACE: a matlab kriging toolbox, version 2.0. Technical report IMM-REP-2002-12 Informatics and Mathematical Modelling, Technical University of Denmark, 2002 http://www2.imm.dtu.dk/projects/dace/.

[21] E. Bayo, J. Gracia. Stiffness modelling of 2D welded joints using metamodels based on mode shapes. Journal of Constructional Steel Research, 156 (2019), 242-251

[22] A. Loureiro, M. Lopez, E. Bayo. Shear behaviour of stiffened double rectangular column panels: Characterization and cruciform element. Journal of Constructional Steel Research, 117 (2016), 126-138.

Annex 1. Validation set of joints for HEAs columns

Model	Column	Left Beam	Right beam	Model	Column	Left Beam	Right beam
1	HE 100 A	IPE 160	IPE 140	47	HE 240 A	IPE 500	IPE 330
2	HE 100 A	IPE 120	IPE 80	48	HE 240 A	IPE 450	IPE 300
3	HE 120 A	IPE 240	IPE 120	49	HE 240 A	IPE 400	IPE 300
4	HE 120 A	IPE 240	IPE 200	50	HE 260 A	IPE 600	IPE 330
5	HE 120 A	IPE 220	IPE 140	51	HE 260 A	IPE 600	IPE 500
6	HE 120 A	IPE 200	IPE 100	52	HE 260 A	IPE 550	IPE 360
7	HE 120 A	IPE 200	IPE 180	53	HE 260 A	IPE 500	IPE 300
8	HE 120 A	IPE 180	IPE 160	54	HE 260 A	IPE 500	IPE 450
9	HE 120 A	IPE 140	IPE 100	55	HE 260 A	IPE 450	IPE 400
10	HE 140 A	IPE 270	IPE 160	56	HE 280 A	IPE 600	IPE 300
11	HE 140 A	IPE 270	IPE 240	57	HE 280 A	IPE 600	IPE 450
12	HE 140 A	IPE 240	IPE 180	58	HE 280 A	IPE 550	IPE 330
13	HE 140 A	IPE 220	IPE 140	59	HE 280 A	IPE 550	IPE 500
14	HE 140 A	IPE 200	IPE 120	60	HE 280 A	IPE 500	IPE 400
15	HE 140 A	IPE 180	IPE 120	61	HE 280 A	IPE 450	IPE 360
16	HE 160 A	IPE 330	IPE 160	62	HE 280 A	IPE 400	IPE 360
17	HE 160 A	IPE 330	IPE 240	63	HE 300 A	IPE 600	IPE 400
18	HE 160 A	IPE 300	IPE 160	64	HE 300 A	IPE 550	IPE 300
19	HE 160 A	IPE 300	IPE 240	65	HE 300 A	IPE 550	IPE 450
20	HE 160 A	IPE 270	IPE 180	66	HE 300 A	IPE 500	IPE 360
21	HE 160 A	IPE 240	IPE 140	67	HE 300 A	IPE 450	IPE 330
22	HE 160 A	IPE 240	IPE 220	68	HE 300 A	IPE 400	IPE 330
23	HE 160 A	IPE 220	IPE 200	69	HE 320 A	IPE 600	IPE 360
24	HE 180 A	IPE 400	IPE 160	70	HE 320 A	IPE 600	IPE 550
25	HE 180 A	IPE 400	IPE 240	71	HE 320 A	IPE 550	IPE 400
26	HE 180 A	IPE 360	IPE 220	72	HE 320 A	IPE 500	IPE 330
27	HE 180 A	IPE 360	IPE 330	73	HE 320 A	IPE 450	IPE 300
28	HE 180 A	IPE 330	IPE 220	74	HE 320 A	IPE 400	IPE 300
29	HE 180 A	IPE 300	IPE 160	75	HE 340 A	IPE 600	IPE 330
30	HE 180 A	IPE 300	IPE 240	76	HE 340 A	IPE 600	IPE 500
31	HE 180 A	IPE 270	IPE 200	77	HE 340 A	IPE 550	IPE 360
32	HE 200 A	IPE 500	IPE 270	78	HE 340 A	IPE 500	IPE 300
33	HE 200 A	IPE 500	IPE 400	79	HE 340 A	IPE 500	IPE 450
34	HE 200 A	IPE 450	IPE 300	80	HE 340 A	IPE 450	IPE 400
35	HE 200 A	IPE 400	IPE 240	81	HE 360 A	IPE 600	IPE 300
36	HE 200 A	IPE 400	IPE 360	82	HE 360 A	IPE 600	IPE 450
37	HE 200 A	IPE 360	IPE 330	83	HE 360 A	IPE 550	IPE 330
38	HE 220 A	IPE 600	IPE 400	84	HE 360 A	IPE 550	IPE 500
39	HE 220 A	IPE 550	IPE 300	85	HE 360 A	IPE 500	IPE 400
40	HE 220 A	IPE 550	IPE 450	86	HE 360 A	IPE 450	IPE 360
41	HE 220 A	IPE 500	IPE 360	87	HE 360 A	IPE 400	IPE 360
42	HE 220 A	IPE 450	IPE 330	88	HE 400 A	IPE 600	IPE 400
43	HE 220 A	IPE 400	IPE 330	89	HE 400 A	IPE 550	IPE 300
44	HE 240 A	IPE 600	IPE 360	90	HE 400 A	IPE 550	IPE 450
45	HE 240 A	IPE 600	IPE 550	91	HE 400 A	IPE 500	IPE 360
6	HE 240 A	IPE 550	IPE 400	92	HE 400 A	IPE 450	IPE 330

Annex 2. Validation set of joints for HEBs columns

Model	Column	Left Beam	Right beam	Model	Column	Left Beam	Right beam
1	HE 100 B	IPE 120	IPE 80	47	HE 240 B	IPE 500	IPE 330
2	HE 120 B	IPE 240	IPE 120	48	HE 240 B	IPE 450	IPE 300
3	HE 120 B	IPE 240	IPE 200	49	HE 240 B	IPE 400	IPE 300
4	HE 120 B	IPE 220	IPE 140	50	HE 260 B	IPE 600	IPE 330
5	HE 120 B	IPE 200	IPE 100	51	HE 260 B	IPE 600	IPE 500
6	HE 120 B	IPE 200	IPE 180	52	HE 260 B	IPE 550	IPE 360
7	HE 120 B	IPE 180	IPE 160	53	HE 260 B	IPE 500	IPE 300
8	HE 120 B	IPE 140	IPE 100	54	HE 260 B	IPE 500	IPE 450
9	HE 140 B	IPE 270	IPE 160	55	HE 260 B	IPE 450	IPE 400
10	HE 140 B	IPE 270	IPE 240	56	HE 280 B	IPE 600	IPE 300
11	HE 140 B	IPE 240	IPE 180	57	HE 280 B	IPE 600	IPE 450
12	HE 140 B	IPE 220	IPE 140	58	HE 280 B	IPE 550	IPE 330
13	HE 140 B	IPE 200	IPE 120	59	HE 280 B	IPE 550	IPE 500
14	HE 140 B	IPE 180	IPE 120	60	HE 280 B	IPE 500	IPE 400
15	HE 160 B	IPE 330	IPE 160	61	HE 280 B	IPE 450	IPE 360
16	HE 160 B	IPE 330	IPE 240	62	HE 280 B	IPE 400	IPE 360
17	HE 160 B	IPE 300	IPE 160	63	HE 300 B	IPE 600	IPE 400
18	HE 160 B	IPE 300	IPE 240	64	HE 300 B	IPE 550	IPE 300
19	HE 160 B	IPE 270	IPE 180	65	HE 300 B	IPE 550	IPE 450
20	HE 160 B	IPE 240	IPE 140	66	HE 300 B	IPE 500	IPE 360
21	HE 160 B	IPE 240	IPE 220	67	HE 300 B	IPE 450	IPE 330
22	HE 160 B	IPE 220	IPE 200	68	HE 300 B	IPE 400	IPE 330
23	HE 180 B	IPE 400	IPE 160	69	HE 320 B	IPE 600	IPE 360
24	HE 180 B	IPE 400	IPE 240	70	HE 320 B	IPE 600	IPE 550
25	HE 180 B	IPE 400	IPE 360	71	HE 320 B	IPE 550	IPE 400
26	HE 180 B	IPE 360	IPE 220	72	HE 320 B	IPE 500	IPE 330
27	HE 180 B	IPE 360	IPE 330	73	HE 320 B	IPE 450	IPE 300
28	HE 180 B	IPE 330	IPE 220	74	HE 320 B	IPE 400	IPE 300
29	HE 180 B	IPE 300	IPE 160	75	HE 340 B	IPE 600	IPE 330
30	HE 180 B	IPE 300	IPE 240	76	HE 340 B	IPE 600	IPE 500
31	HE 180 B	IPE 270	IPE 200	77	HE 340 B	IPE 550	IPE 360
32	HE 200 B	IPE 500	IPE 270	78	HE 340 B	IPE 500	IPE 300
33	HE 200 B	IPE 500	IPE 400	79	HE 340 B	IPE 500	IPE 450
34	HE 200 B	IPE 450	IPE 300	80	HE 340 B	IPE 450	IPE 400
35	HE 200 B	IPE 400	IPE 240	81	HE 360 B	IPE 600	IPE 300
36	HE 200 B	IPE 400	IPE 360	82	HE 360 B	IPE 600	IPE 450
37	HE 200 B	IPE 360	IPE 330	83	HE 360 B	IPE 550	IPE 330
38	HE 220 B	IPE 600	IPE 400	84	HE 360 B	IPE 550	IPE 500
39	HE 220 B	IPE 550	IPE 300	85	HE 360 B	IPE 500	IPE 400
40	HE 220 B	IPE 550	IPE 450	86	HE 360 B	IPE 450	IPE 360
41	HE 220 B	IPE 500	IPE 360	87	HE 360 B	IPE 400	IPE 360
42	HE 220 B	IPE 450	IPE 330	88	HE 400 B	IPE 600	IPE 400
43	HE 220 B	IPE 400	IPE 330	89	HE 400 B	IPE 550	IPE 300
44	HE 240 B	IPE 600	IPE 360	90	HE 400 B	IPE 550	IPE 450
45	HE 240 B	IPE 600	IPE 550	91	HE 400 B	IPE 500	IPE 360
46	HE 240 B	IPE 550	IPE 400	92	HE 400 B	IPE 450	IPE 330